



Crystal structure, thermal, redox, and EPR studies of copper(II) complexes with catechol-based quaternary ammonium salts

Azamat Bikmukhametov ^a , Maksim Zhernakov ^b , Mikhail Bukharov ^a ,
Yury Kuzin ^a , Daut Islamov ^c , Artur Khannanov ^a , Alexander Gerasimov ^a ,
Liana Zubaidullina ^a , Alexander Rodionov ^d , Pavel Padnya ^{a,*} , Ivan Stoikov ^{a,*}

a: A.M. Butlerov Chemical Institute, Kazan Federal University , Kazan 420008, Russia

b: Institute of Inorganic and Analytical Chemistry, Justus Liebig University Giessen , Giessen 35392, Germany

c: Laboratory for structural analysis of biomacromolecules, FRC Kazan Scientific Center of the Russian Academy of Sciences , Kazan 420008, Russia

d: Institute of Physics, Kazan Federal University , Kazan 420008, Russia

* Corresponding authors: padnya.ksu@gmail.com (P.P.); ivan.stoikov@mail.ru (I.S.).

Abstract

Quaternary ammonium salts (QASs), acylhydrazones and catechols are well known for their antimicrobial, antioxidant and antitumor properties. Complexation of acylhydrazones and catechols with Cu(II) ions potentially leads to obtaining compounds with promising biological properties. In this paper, we present a synthesis of two binuclear copper(II) complexes based on redox-active QASs with acylhydrazone and catechol fragments and a study of their structure in the solid state. The copper(II) complex with a tributylammonium fragment crystallizes in the triclinic space group $P\bar{1}$ with the following lattice parameters: $a = 10.1459(5) \text{ \AA}$, $b = 15.1239(7) \text{ \AA}$, $c = 16.3279(5) \text{ \AA}$, $\alpha = 110.231(4)^\circ$, $\beta = 104.689(4)^\circ$, $\gamma = 101.637(4)^\circ$. The structure exhibits binuclear nature, showing the distance Cu–Cu of 3.507 \AA , and Jahn-Teller distortions with large elongation along the axial positions. The thermal stability of the ligands was found to be higher than that of the corresponding complexes up to 66–77 °C. EPR spectroscopy proved the dissociation of the complexes in the methanol solution into the monomeric forms. Complexation with Cu(II) cation shifted oxidation peaks of the ligands towards the lower potentials. The target compounds may be applied to create selective systems for metal ion separation, and may also possess potential antimicrobial, antioxidant, and antitumor properties.

Key findings

- Acylhydrazone-based redox-active catechol-based quaternary ammonium salts formed a binuclear complex with Cu(II) cation in the solid state.
- Complexation with Cu(II) ions lowered thermal stability and shifted potentials by 60–70 mV for the first and 350–400 mV for the second anodic peaks of the ionic liquids
- The structure exhibits a binuclear nature, showing the distance Cu–Cu of 3.507 \AA

© 2026, the Authors. This article is published in open access under the terms and conditions of the Creative Commons Attribution (CC BY) license (<http://creativecommons.org/licenses/by/4.0/>), which permits unrestricted re-use of the work in any medium provided the original work is properly cited.

1. Introduction

Quaternary ammonium salts (QASs) are widely used as surfactants, antimicrobial agents, and mass transfer catalysts [1]. One of the most promising areas of their application is the synthesis of ionic liquids (ILs) – salts with a melting

point below 100 °C. The connection between QASs and ILs is due to the ability of bulky, asymmetric quaternary ammonium cations, in combination with large, non-coordinating anions (e.g., BF_4^- , PF_6^- , NTf_2^-), to hinder crystallization, which leads to a lower melting point [2]. These com-

Accompanying information

Article history

Received: 23.04.2026

Revised: 30.04.2026

Accepted: 02.05.2026

Available online: 02.05.2026

Keywords

Copper(II) complex, acylhydrazones, catechols, quaternary ammonium, redox activity, crystal structure

Funding

This work was financially supported by Russian Science Foundation (Grant No. 24-73-10079, <https://rscf.ru/en/project/24-73-10079/>).

Supplementary information

Supplementary materials:

Transparent peer review:

Sustainable Development Goals



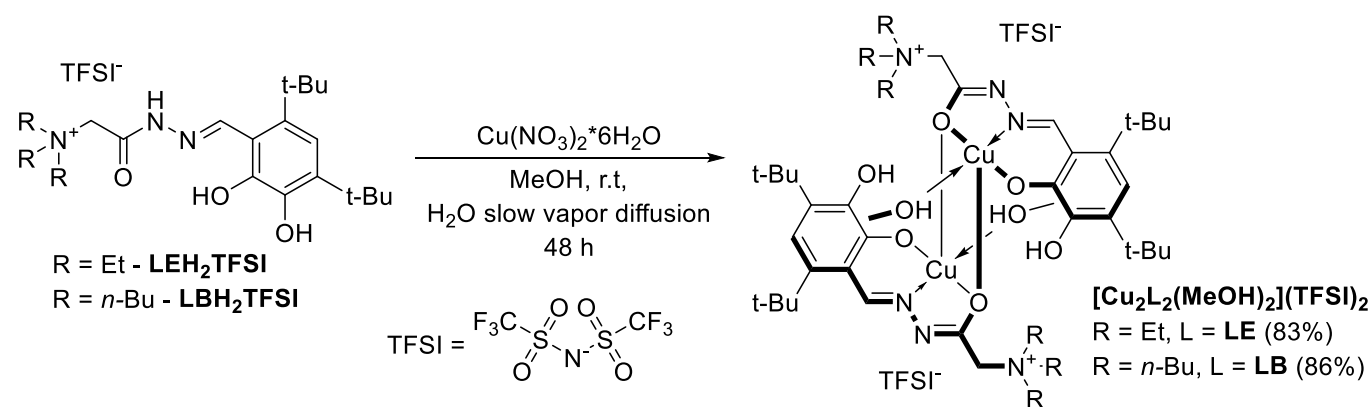
pounds possess a unique combination of properties: negligible vapor pressure, high thermal and chemical stability, a broad electrochemical window, and, most importantly, the ability to vary the cation-anion composition to achieve desired characteristics [2]. As a result, ILs are in high demand in numerous applications—including catalysis [3, 4], electrolytes [5, 6], and reaction media [4, 7], as well as selective extraction systems [4, 8], biomedicine [9], and industry [10, 11].

Further development of the concept of ionic liquids has led to the creation of task-specific ILs – functionalized derivatives bearing additional groups capable of achieving the target properties [12]. Unlike classic ILs, such compounds are not intended for large-scale utilization but for use as functional materials, given their high cost and unique properties. The increased complexity of their structures compared to classic ILs often has a negative impact on their thermal properties. Hence, their melting points can be significantly higher than those of conventional ILs, and may even exceed 100 °C [13 – 15]. In recent years, the biomedical applications of ILs have been actively developing, including their use as active pharmaceutical ingredients (so-called API-ILs) [16 – 18], drug delivery systems [19 – 21], and antimicrobial agents [22–24]. In addition, the unique solvation ability of ILs enables the creation of selective systems for the recognition and separation of biologically significant molecules like alkaloids, terpenoids, and flavonoids [11], organic compounds (via gas and liquid chromatography or electrophoresis) [25–27], and metal ions (e.g., Hg(II), Cd(II), and rare-earth element ions) [28, 29]. To improve the selectivity of such systems, additional structural fragments capable of forming complexes with specific metal ions can be incorporated into the IL structure, leading to the emergence of task-specific ILs [30, 31].

Structural fragments that can ensure selective complexation are a catechol group and an acylhydrazone moiety. Catechols are well known for their capability of complexing transition metal ions. In particular, we can highlight examples of chelation of Fe(III) [32 – 34], Cu(II) [34] and Zn(II) [34] by the related ligands. Acylhydrazones are also capable of forming complexes with *d*-metal cations, such as Cu(II)

[35 – 38], Ni(II) [36 – 39], Co(II) [38, 39], Zn(II) [36, 38], and Cd(II) [36, 39]. The combination of acylhydrazone and catechol moieties within a single structure can be conveniently achieved using 2,3-dihydroxybenzaldehyde derivatives, leading to the formation of compounds capable of forming mononuclear [40] and, predominantly, binuclear [41 – 49] complexes with tridentate coordination by the acylhydrazone in the imidol form and one of the OH-groups of the catechol fragment. However, the data on copper(II) complexes with ligands based on QASs with acylhydrazone and catechol moieties is very limited and represented by only two examples in the CSD databank [50, 51].

The biological properties of the derivatives of each individual fragment have been extensively studied. Acylhydrazones often exhibit antitumor [52 – 54], antimicrobial [55 – 57], antiparasitic [58 – 60], and anti-inflammatory [61 – 63] properties. Catechol derivatives often possess antioxidant [64 – 66] and adhesive [67 – 69] properties. QASs are widely known for their antimicrobial properties [70 – 72]. The combination of these functional groups in a single structure can lead to compounds with combined or improved properties compared to substances containing the moieties separately. As demonstrated in numerous studies by the group of A. Bogdanov, acylhydrazones combining a catechol and/or quaternary ammonium moiety in their structure may exhibit pronounced antimicrobial [73 – 81], anticoagulant [73, 75], antioxidant [76] activity, and are also capable of inhibiting certain enzymes, such as butyrylcholinesterase [82]. In addition, the formation of complexes with copper(II) ions can enhance certain biological properties. The literature contains examples of studies in which copper complexes of compounds exhibited higher cytotoxicity [83 – 86] and more pronounced antimicrobial [87, 88] properties. Moreover, copper chelators are widely used for the treatment of conditions related to impaired copper metabolism in the human body, such as Wilson's disease [89] and Menkes disease [90]. Studying the structure of such compounds will help establish a relationship between structure and properties, enabling the targeted design of systems and materials with desired properties.



Scheme 1 Synthesis of the target complexes.

In this study, we synthesized two novel copper(II) complexes of catechol-based QASs and comprehensively studied them with structural, thermal, electrochemical, and EPR techniques. The target compounds may open up the possibility of creating selective systems for metal ion separation and may also possess potential antimicrobial, antioxidant, and antitumor properties.

2. Experimental

2.1. Reagents

Acylhydrazones **LEH₂TFSI** and **LBH₂TFSI** (Scheme 1) were synthesized according to the literature procedures [91]. Methanol and Cu(NO₃)₂·6H₂O were purified by standard procedures. Lithium perchlorate was purchased from Acros (Fair Lawn, NJ, USA).

2.2. Synthesis of complexes

All complexes were obtained according to the general procedure (Scheme 1). Acylhydrazone ligands **LEH₂TFSI** or **LBH₂TFSI** in an amount of 0.065 mmol with 29 mg (20% molar excess) of Cu(NO₃)₂·6H₂O were dissolved in 5 ml MeOH in a glass vial. The vials with the resulting dark green solutions were left with the beaker of water (~50 ml) and covered with a large beaker for slow vapor diffusion. The system was left for 48 h. The resulting dark green crystals were filtered off and washed with distilled water, yielding the target complexes **[Cu₂(LE)₂(MeOH)₂](TFSI)₂** (42.1 mg, 83%) and **[Cu₂(LB)₂(MeOH)₂](TFSI)₂** (56.2 mg, 86%). In the case of the complex with the ligand **LB**, the crystals formed were suitable for single-crystal X-ray diffraction.

2.3. Single crystal X-ray diffraction

Data set for the single crystal of **[Cu₂(LB)₂(MeOH)₂](TFSI)₂** was collected on a Rigaku Xta-Lab Synergy S instrument with a HyPix detector and a PhotonJet microfocuss X-ray tube using Cu-K α (1.54184 Å) radiation at room temperature. Images were indexed and integrated using the CrysAlisPro data reduction package. Data were corrected for systematic errors and absorption using the ABSPACK module: numerical absorption correction based on Gaussian integration over a multifaceted crystal model, and empirical absorption correction based on spherical harmonics according to the point group symmetry using equivalent reflections was applied. The GRAL module was used for the analysis of systematic absences and space group determination. The structure was solved by direct methods using SHELXT [92] and refined by the full-matrix least-squares on F² using SHELXL [93]. Non-hydrogen atoms were refined anisotropically. The hydrogen atoms were inserted at the calculated positions and refined as riding atoms. The figures were generated using Mercury 4.1 [94] program. Crystallographic data and structural refinements are summarized in Table S1.

2.4. Powder X-ray diffraction

Powder X-ray diffraction (PXRD) studies were made using a MiniFlex 600 diffractometer (Rigaku, Japan) equipped with a D/teX Ultra detector. In this experiment, Cu-K α radiation (30 kV, 15 mA) was used, and data were collected at room temperature in the range of 2 θ from 3 to 100° with a step of 0.02° and exposure time at each point of 0.24 s without sample rotation.

2.5. FTIR ART spectroscopy

The FTIR ATR spectra were recorded on the Spectrum 400 FT-IR spectrometer (Perkin-Elmer, Seer Green, Llantrisant, UK) with the Diamond KRS-5 attenuated total internal reflectance attachment (resolution 0.5 cm⁻¹, accumulation of 64 scans, recording time 16 s in the wavelength range 400–4000 cm⁻¹).

2.6. Thermal analysis

Simultaneous thermogravimetry (TG) and differential scanning calorimetry (DSC) of solid samples were performed using the thermoanalyzer STA 449F1 Jupiter (Netzsch, Germany) at the temperature range of 40–500 °C. The measurements were carried out in aluminum crucibles in a dynamic argon atmosphere (75 mL/min) at a temperature scanning rate of 10 °C/min. The weights of the sample were 4.9–10.2 mg.

2.7. EPR spectroscopy

X-band EPR spectra were recorded with ESP 300 spectrometer at room temperature and simulated using EasySpin software package (version 6.0.12) [95]. For recording the EPR spectra, 2 thin tubes (1 mm outer diameter) with the samples were placed inside a single 5 mm diameter tube.

2.8. Electrochemical measurements

Electrochemical investigation was performed using potentiostat - galvanostat CHI 440B (CH Instruments, Austin, USA) with a stationary three-electrode cell at room temperature. Glassy carbon electrode, 2 mm in diameter, was used as a working electrode, Ag/AgCl (1 M NaCl) (CHI128) - as reference electrode, and Pt wire (CHI 129) was used as counter electrode. Before the experiment, the working electrode was polished on silicon carbide grinding paper (P10000), followed by rinsing with water and ethanol. Purity of the electrode surface was controlled by recording the background voltammograms. 0.1 M LiClO₄ in methanol was used as a working solution. Three cycles were recorded in the range of [-200; 2000] mV, the initial potential was 200 mV, scan rate was 100 mV/s.

3. Results and discussion

3.1. Structural study

The compound $[\text{Cu}_2(\text{LB})_2(\text{MeOH})_2](\text{TFSI})_2$ crystallizes in the triclinic space group $P\bar{1}$, exhibiting a binuclear structure consisting of the complex cation $[\text{Cu}_2(\text{LB})_2(\text{MeOH})_2]^{2+}$ and bistriflimide anions (Figure 1). The asymmetric unit $[\text{Cu}(\text{LB})(\text{MeOH})]^+$ of the crystal structure is sitting on an inversion center; thus, forming a dimer via the symmetry operation $(-x; -y; -z)$, with the copper atoms being symmetry equivalents. Considering the asymmetric unit, the copper atom is coordinating one methanol molecule and one ligand molecule via N and O atoms of an acylhydrazone part and O atom of a phenol part. This environment forms square planar coordination, and the second ligand LB related by the inversion center fulfills the coordination sphere, completing a square-pyramidal polyhedron via the O atom of an acylhydrazone group. Thus, this oxygen atom serves as a bridging one, enabling the formation of a dimeric structure.

Given the considerations above, we can infer that both copper atoms in the binuclear cation exhibit a coordination number of five and a square-pyramidal coordination environment. Thus, the coordination polyhedra are connected by a shared edge, forming a binuclear structure. To analyze the coordination environment in detail, we present Figure 2, which shows a closer look at the neighboring atoms and selected interatomic distances. Remarkably, the interatomic distance between the Cu atom and the O atom of the TFSI anion (2.884(3) Å) falls into a 3 Å range, indicating a so-called short contact between them. This can be considered as an additional coordinated ligand, although the distance is even larger than that between the Cu atom and the O atom from the symmetry-related ligand (2.707(3) Å). Therefore, we can conclude that the second ligand and the TFSI anion are coordinated rather weakly.

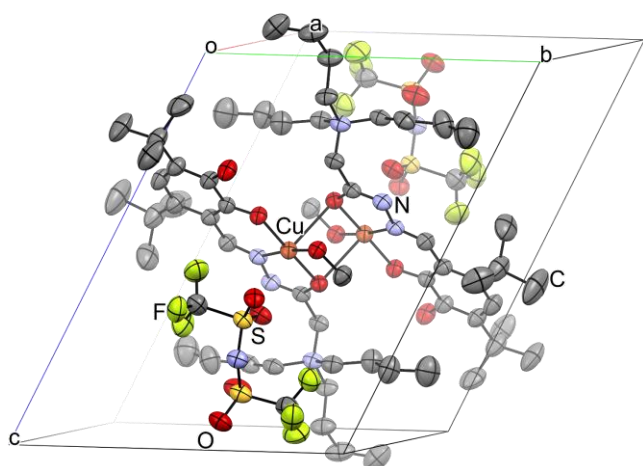


Figure 1. A unit cell of the compound $[\text{Cu}_2(\text{LB})_2(\text{MeOH})_2](\text{TFSI})_2$ is presented along the a axis with a 45° rotation around the vertical axis. Color code: Cu - orange; S - yellow; F - green; O - red; N - blue; C - gray. Hydrogen atoms are omitted for clarity. Thermal ellipsoids represent 30% level probability of atom positions.

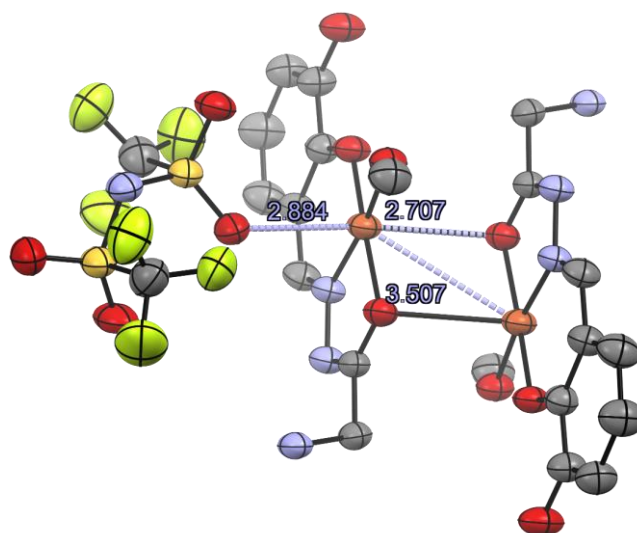


Figure 2 Excerpt of the crystal structure of the compound $[\text{Cu}_2(\text{LB})_2(\text{MeOH})_2](\text{TFSI})_2$. The distance $\text{Cu}-\text{O}_{\text{TFSI}}$ is 2.884(3) Å, the distance $\text{Cu}-\text{O}_{\text{LB}}$ is 2.707(3) Å, and the distance $\text{Cu}-\text{Cu}$ is 3.5067(8) Å. n-Butyl and tert-Butyl moieties, as well as hydrogen atoms, are omitted for clarity.

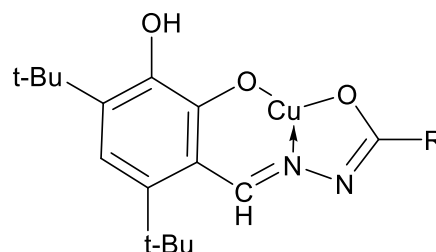


Figure 3 A coordination site of Cu in the compound $[\text{Cu}_2(\text{LB})_2(\text{MeOH})_2](\text{TFSI})_2$. A quaternary ammonium fragment, MeOH, and a symmetry related ligand are omitted for clarity.

A conducted review of the CSD database revealed that these axial interatomic distances are larger than in related binuclear structures, exhibiting an acylhydrazone moiety. For instance, comparable axial Cu–O distances in the CSD database have a mean value of 2.43(5) Å [96 – 98]. In particular, the similar pattern of binuclear nature and large axial distances were reported for the compounds $[\text{Cu}(\text{L})(\text{EtOH})]_2 \cdot 2\text{H}_2\text{O}$ (L = 2-[(2-hydroxy-3-methoxyphenyl)methylideneamino]benzenesulfonic) and $[\text{Cu}(\text{HL})\text{OAc}]_2$ (HL = 2-[2-hydroxyphenyl]-4,4-diphenyl-1,2-dihydro-4H-3,1-benzoxazine), which crystallize in the $P2_1/n$ and $P\bar{1}$ space groups, respectively [96, 99]. Although these ligands are classic Schiff bases without an acylhydrazone fragment, the coordination motif is closely related to our case with a six-membered ring formed by the imine N atom and the phenol O atom (Figure 3). On the contrary, the interatomic distances of the equatorial plane in $[\text{Cu}_2(\text{LB})_2(\text{MeOH})_2](\text{TFSI})_2$ are in the literature range with the mean value of 1.95(3) Å [50, 51, 96–98]. This applies to coordination compounds containing acylhydrazone and catechol moieties, exhibiting the same coordination site as shown in Figure 3. In particular, it was observed for $[\text{Cu}(\text{HL})(\text{MeOH})]_2$ (HL = (E/Z)-4-(2-(1-cyano-2-ethoxy-2-oxoethylidene)hydrazinyl)-3-hydroxybenzoic acid and

[Cu₂(L)₂(DMSO)(MeOH)] (L = *N'*-(4-(diethylamino)-2-hydroxybenzylidene)-1-naphthohydrazide, which showed equatorial distances in the range of [1.913(2)–1.923(2) Å] and [1.912(2)–1.930(2) Å], respectively [97–98].

Having the interatomic distances in the equatorial plane less than 2 Å and elongated ones (>2.5 Å) in the axial plane, the pronounced Jahn-Teller effect drives a lowering in symmetry of the coordination environment [100]. In particular, the symmetry decreases from octahedral coordination, point group *O_h* in the perfect case, to square-pyramidal, the point group *C_{4v}*, if the O atom from the symmetry-related ligand is considered bound to the Cu atom, or to the square-planar one, the point group *D_{4h}* if not. Consequently, we expect the binuclear structure to exist only in the solid state or concentrated solutions and rapidly exchange axial ligands in substitution reactions. This type of distortion is common for copper(II) complexes [38, 101], and a conducted review revealed a study describing the kinetic effects of such reactions with different N-donors and amino acids [84].

Since the structure is binuclear and the Cu²⁺ ion is magnetically active due to the 3d⁹ configuration, magnetic interactions between the Cu atoms may be expected. As Figure 2 shows, the distance between the Cu atoms is 3.5067(8) Å, which is considered sufficient for such interactions [98, 102, 103].

Powder diffraction technique was used to study the phase composition of the obtained sample. Figure S1 shows the comparison of the experimental and simulated powder patterns, which indicates the presence of multiple phases in it. Although the sample was initially isolated as single crystals suitable for structure determination, it proved to be unstable upon storage outside the mother liquor. Nonetheless, the first three peaks of the simulated powder pattern are still visible in the experimental one, showing a significant decrease in intensities and indicating a transformation of the sample. The broadening and overlapping of the other reflections support this inference, as well. Since the recrystallization of the unsolvated complex is questionable, the only option remaining is to determine the structure of a completely dried powder sample. However, this is challenging for such complex and low-symmetry structures.

A comparison of the IR spectra of ligands and the corresponding complexes reveals a shift in several absorption bands (Figure 4). A new absorption band at 3503–3579 cm⁻¹ corresponds to hydrogen-bond vibrations from the methanol molecule included in the complex. The band corresponding to the hydrogen bond vibrations of the ligand phenolic group at 3427–3430 cm⁻¹ has shifted to the area of 3393–3414 cm⁻¹, while the band at 3280 cm⁻¹ corresponding to the N-H bond vibrations of the amide fragment disappeared due to amide-imidol tautomerization upon complex formation [36]. Furthermore, the tautomerization of the ligand's amide moiety is confirmed by the disappearance of the band at 1688–1696 cm⁻¹ (C=O bond vibrations

in the amide moiety of the ligand), the appearance of the band at 1527 cm⁻¹ (vibrations of the C=N=N=C moiety of the complex), as well as the appearance of new bands at 1296–1303 cm⁻¹ and 1089–1104 cm⁻¹ (vibrations of the C–O–bond). In addition, the appearance of a new band at 481–487 cm⁻¹ can be attributed to characteristic Cu–O or Cu–N bond vibrations, as it was assigned in similar structures [104, 105].

3.2. Thermal properties study

The thermal properties of the obtained complexes were investigated by simultaneous thermogravimetry-differential scanning calorimetry (TG-DSC). As shown in Figure 5, both complexes lost their methanol molecules upon mild heating, and complete methanol loss occurs at temperatures of 110–130 °C. For both complexes, the experimental mass loss is slightly less than the theoretical value. For **[Cu₂(LE)₂(MeOH)₂](TFSI)₂**, the experimental value was 3.7% compared to the theoretical 4.1%. In the case of the **[Cu₂(LB)₂(MeOH)₂](TFSI)₂** complex, the experimental mass loss was only 1.3% compared to 3.7% in the theoretical estimate. This difference can be attributed to the partial loss of methanol from the coordination sphere during storage.

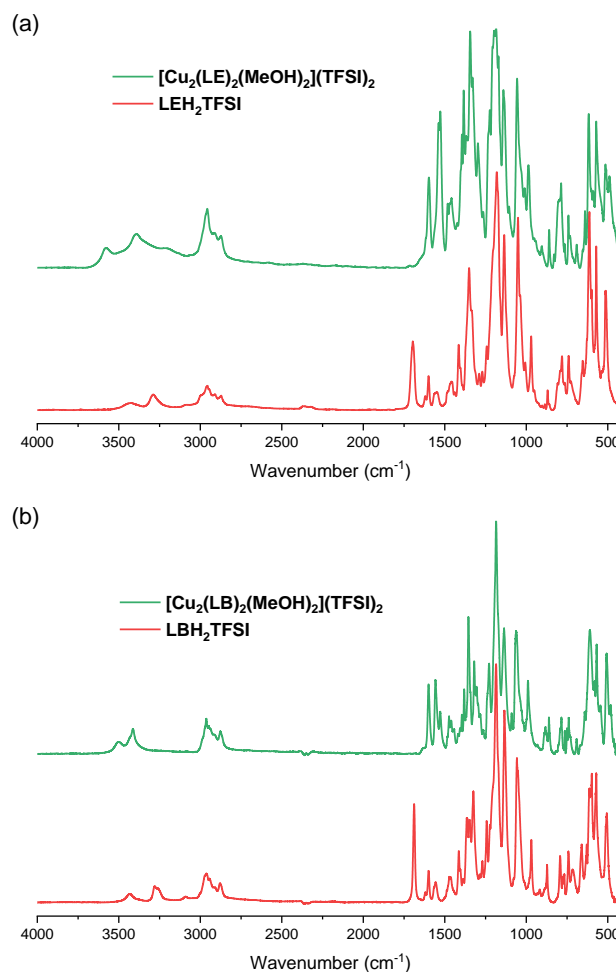
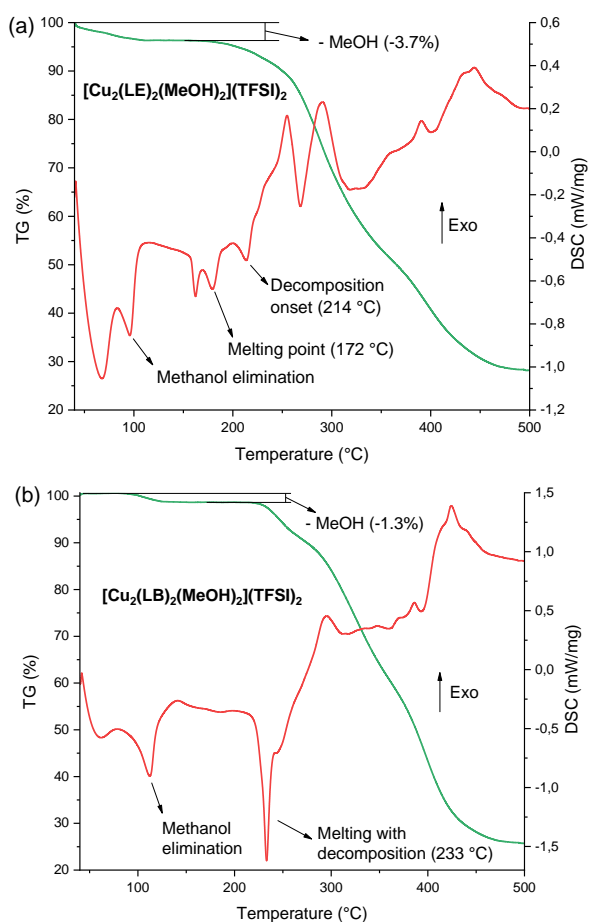


Figure 4 Comparison of normalized FTIR ART spectra of (a) **LEH₂TFSI** and **[Cu₂(LE)₂(MeOH)₂](TFSI)₂**, (b) **LBH₂TFSI** and **[Cu₂(LB)₂(MeOH)₂](TFSI)₂** in solid state.

Table 1 Melting and decomposition points of ligands and corresponding copper(II) complexes according to TG/DSC data.

Compound	Melting point (°C)	Decomposition point (°C)	Reference
LEH ₂ TFSI	184	291	[91]
LBH ₂ TFSI	203	300	[91]
[Cu ₂ (LE) ₂ (MeOH) ₂](TFSI) ₂	172	214	This work
[Cu ₂ (LB) ₂ (MeOH) ₂](TFSI) ₂	233 ^a	233 ^a	This work

^a Melting with decomposition.**Figure 5** TG (green)/DSC (red) curves of (a) [Cu₂(LE)₂(MeOH)₂](TFSI)₂ and (b) [Cu₂(LB)₂(MeOH)₂](TFSI)₂.

Comparing the DSC curves for both complexes, several variations can be observed, presumably related to structural differences in the cationic fragments. For the complex [Cu₂(LE)₂(MeOH)₂](TFSI)₂ with the less sterically hindered triethylammonium fragment, in addition to the endo-effects associated with the removal of methanol from the coordination sphere, a peak at 162 °C is observed, which can presumably be attributed to a solid-solid phase transition. An endo-effect at 233 °C corresponding to melting with decomposition is present on the DSC curve of the compound [Cu₂(LB)₂(MeOH)₂](TFSI)₂. No separate melting peak or solid-solid transition is observed, which can be explained by the lower mobility of the ligand due to the steric hindrance of the tributylammonium fragment. The melting and decomposition temperatures of the ligands and the corresponding copper(II) complexes are given in Table 1. The

data show that the coordination with Cu²⁺ ions leads to a significant decrease in the decomposition temperature by 67 °C for [Cu₂(LB)₂(MeOH)₂](TFSI)₂ and 77 °C for [Cu₂(LE)₂(MeOH)₂](TFSI)₂. The thermal stability of similar compounds is poorly represented in the literature, and the melting and decomposition temperatures for such complexes are often not considered critically significant. A study of copper(II) complexes with comparable hydrazone ligands shows that partial solvent loss in the solid state occurs even at temperatures of -15 °C, leading to changes in their powder X-ray diffractograms [46]. For complexes with methanol in the coordination sphere, complete solvent removal was observed at temperatures of 108–176 °C, and irreversible decomposition with significant mass loss began in the temperature range of 268–300 °C, which is significantly higher than the values in our work. This difference in decomposition temperatures may be attributed to the presence of a hydroxyl group at the 3-position of the aromatic ring, which significantly facilitates the oxidation and decomposition of the ligand due to the conjugation disruption of the aromatic ring in the quinone form.

3.3. EPR study of the copper complex

The EPR spectra of methanolic solutions of 5.0 mM [Cu₂(LB)₂(MeOH)₂](TFSI)₂ (Figure 6) and 1.0 mM [Cu₂(LE)₂(MeOH)₂](TFSI)₂ (Figure S2) correspond to mononuclear copper(II) complexes. The parameters of the spectra are given in Table S2. The spectra display four hyperfine lines, which is a characteristic of Cu²⁺ ions with a nuclear spin of $I = 3/2$. Superhyperfine splitting is clearly observed on the fourth line due to the interaction of the unpaired electron with the coordinated nitrogen atom of the ligand, confirming the formation of a 1:1 complex in solution. The second-derivative spectrum also reveals weak hyperfine coupling with the second nitrogen atom of the ligand and hydrazone moiety (Figure S3). Thus, EPR data indicate that the binuclear [Cu₂(LB)₂(MeOH)₂](TFSI)₂ and [Cu₂(LE)₂(MeOH)₂](TFSI)₂ complexes dissociate in methanol solution into the mononuclear Cu(II) species [Cu(LB)(MeOH)₂]TFSI and [Cu(LE)(MeOH)₂]TFSI respectively, as it was presumed at the section 3.1. Such a dissociation was also observed in DMSO solution for similar binuclear Cu(II) compounds with acylhydrazone ligands [43, 44], the solution EPR spectra of which are typical for mononuclear complexes.

3.4. Redox activity of the obtained complexes

Although the EPR data proved that target binuclear complexes [Cu₂L₂(MeOH)₂]TFSI₂ do dissociate in solution, electrochemical studies of the obtained complexes in methanol were performed. In this section, solutions obtained by dissolving [Cu₂L₂(MeOH)₂]TFSI₂ complexes in methanol will be referred to as solutions of dissociated complexes [Cu(LB)(MeOH)₂]TFSI with a molar concentration twice that which would result for a binuclear complex in the absence of dissociation.

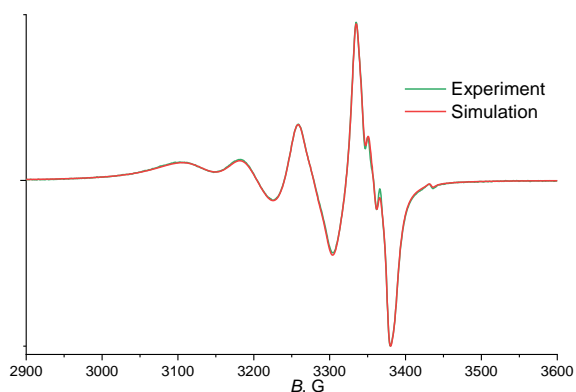


Figure 6 Experimental and simulated EPR spectra of 5.0 mM $[\text{Cu}_2(\text{LB})_2(\text{MeOH})_2](\text{TFSI})_2$ in methanol solution at room temperature. The small signal near 3430 G belongs to a reference radical.

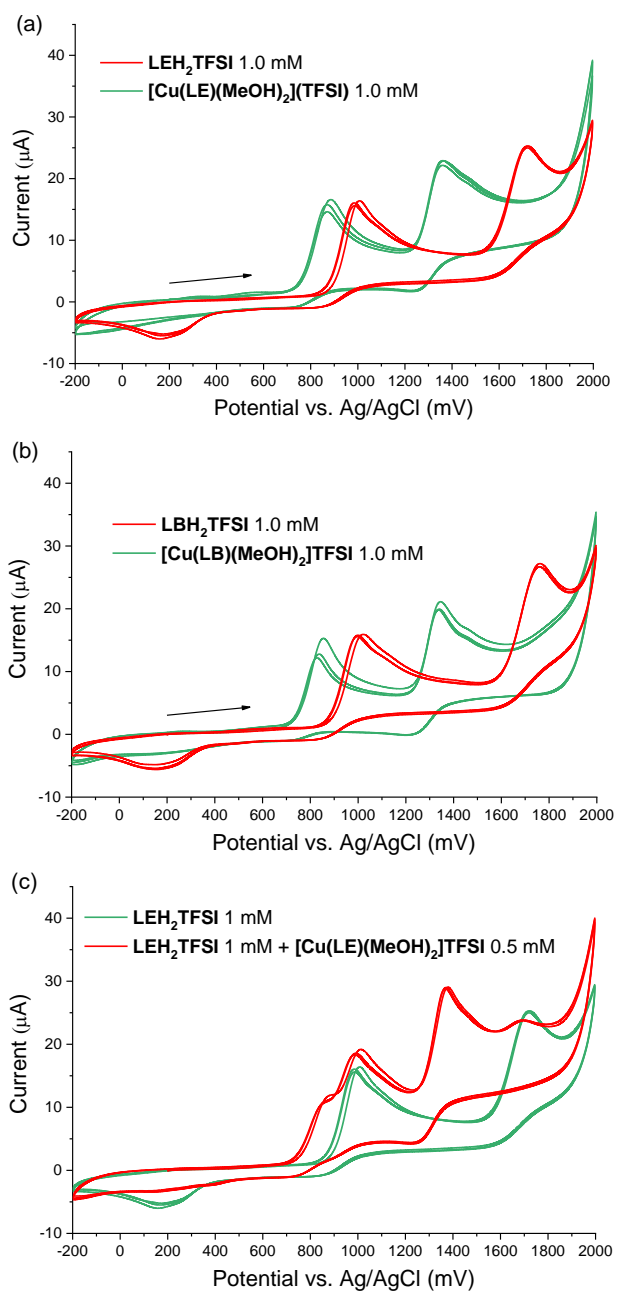


Figure 7 Cyclic voltammograms of (a) $[\text{Cu}(\text{LE})(\text{MeOH})_2]\text{TFSI}$; (b) $[\text{Cu}(\text{LB})(\text{MeOH})_2]\text{TFSI}$; (c) LEH_2TFSI before and after the addition of $[\text{Cu}(\text{LE})(\text{MeOH})_2]\text{TFSI}$ (working solution - 0.1 M LiClO_4 in methanol, potential range [-200; 2000] mV, scan rate 100m V/s).

Cyclic voltammograms (CVs) of the ligands were previously recorded in acetonitrile [91] and a water-acetonitrile mixture (50%, v/v) [106]. Replacing the acetonitrile with methanol did not affect the voltammograms of LEH_2TFSI and LBH_2TFSI (Figure 7a,b). Two oxidation peaks and one reduction peak were recorded, indicating the electrochemical irreversibility of the electrode process. CVs of the copper(II) complexes are also shown in Figure 7a,b. The studied ligands retained their ability to undergo electrochemical transformation. However, the shift in redox peak potentials of the complexes was revealed compared to the signals of free ligands. Electrochemical oxidation of the ligands in the complex occurs at lower potentials. Thus, the shift of the first oxidation peak for $[\text{Cu}_2(\text{LE})_2(\text{MeOH})_2](\text{TFSI})_2$ was about 120 mV and about 60 mV for $[\text{Cu}_2(\text{LB})_2(\text{MeOH})_2](\text{TFSI})_2$. The shift of the second oxidation peak was 350 and 400 mV, respectively.

In order to confirm the absence of the studied complex influence on the reference electrode potential, additional experiments were performed. CVs of LEH_2TFSI solution before and after the addition of aliquot of $[\text{Cu}(\text{LE})(\text{MeOH})_2]\text{TFSI}$ are shown in Figure 7c. Indeed, the resulting voltammograms show the appearance of the previously described peaks of the complex, while the positions of LEH_2 signals remain constant.

Numerous complexes of catechol, benzoquinone, and their derivatives with metal ions such as manganese [107], nickel [108], aluminum [109], iron [110], titanium [111], copper [112], etc. are known from the literature. The nature of the ligand largely determines the redox characteristics of the studied complexes. Thus, Tembwe et al. [113] demonstrated the change in formal redox potential of (diphenylphosphino)ethanecatecholate nickel complex upon varying the nature of the substituent in catechol ligand. The change of almost 200 mV was recorded upon replacing the donor *tert*-butyl fragment with a fluoride one. In [114], the stability of copper(II) complexes with 3,5-di-*tert*-butylcatechols and 3,5-di-*tert*-butyl-*o*-semiquinones formed during the electroreduction of mixtures of copper(II) and 3,5-di-*tert*-butyl-*o*-benzoquinone at mole ratios of 1:2 in acetonitrile or dimethyl sulfoxide was demonstrated. In this case, the addition of metal ions to the ligand solution led to a shift in potentials of both reduction peaks toward positive potentials (by almost 300 mV for the first peak and 1000 mV for the second relative to the peak of the free ligand). Similar behavior was recorded for aluminum- and titanium-catecholate complexes in water, where the oxidation peak of the complex occurred at less positive potentials compared to free catechol [109, 111]. Our data are consistent with the examples given. Thus, the presence of electron-withdrawing fragments in the catechol core determined the significant positive shift in peak potentials compared to catechol [115]. Comparison of first oxidation peak potentials, corresponding to the catechol / semiquinone transition, for $[\text{Cu}(\text{LB})(\text{MeOH})_2]\text{TFSI}$ studied in this article (435 mV vs. Fc^+/Fc couple) and for $[\text{Cu}^{\text{II}}(3,6\text{-Cat})(\text{bipy}^{\text{tBu}})]\cdot\text{THF}$ studied

by Pashanova et al. [112] containing 4,4'-di-*tert*-butyl-2,2'-bipyridyl and 3,6-di-*tert*-butyl-catechol ligands (-345 mV vs. Fc⁺/Fc couple) emphasizes the above-mentioned influence of the ligand nature.

4. Limitations

The main limitations of this research are related to the complex being unstable when stored outside the mother liquor, which hinders it from preserving the phase purity. The study of the properties of the binuclear complexes, as well as their applications, in solution is not feasible due to their dissociation into their monomeric form. Furthermore, this study does not include investigations of potential biological properties. Given the new data on the stability of the complexes, additional studies will be required to investigate these properties, taking into consideration their dissociation in diluted solutions.

5. Conclusions

In this work, we present two novel copper(II) complexes of redox-active ionic liquids containing acylhydrazone and catechol fragments. The target complexes were characterized by single-crystal and powder X-ray diffraction, FTIR ATR spectroscopy, and TG-DSC analysis. According to X-ray crystallography data, the solid-state complex with the tributylammonium ligand crystallizes in the triclinic space group $P\bar{1}$, showing a binuclear nature with a square-pyramidal coordination center. The Cu–Cu distance appeared to be 3.507 Å, suggesting coupling interactions between them in the solid-state. FTIR ATR spectroscopy showed that during complex formation for both ligands, amide-imidol tautomerization of the acylhydrazone fragment occurs, followed by deprotonation and the formation of Cu–O bonds. The dimeric nature of the complex, with its elongated axial bonds (2.707(3) Å), led to the hypothesis that the binuclear form exists exceptionally in the solid state or at most in concentrated solutions and dissociates in diluted ones. EPR spectroscopy in methanol solution proved the dissociation of the binuclear complex into a monomeric form. Superhyperfine splitting on the fourth line corresponds to the interaction of the unpaired electron with the coordinated nitrogen atom of the ligand, confirming the formation of a 1:1 monomeric complex in solution. The effect of binding with Cu(II) ions on the properties of the initial ionic liquids was determined. The thermal stability of the resulting complexes was found to be significantly lower than that of their corresponding ligands. The decomposition points of the complexes were 67–77 °C lower than those of their corresponding ligands. Cyclic voltammetry of the dissociated mononuclear complexes in methanol showed a shift in the potentials of the ligands' anodic peaks by 60–120 mV for the first peak oxidation and by 350–400 mV for the second one. Presumably, such changes could be related to the catalytic properties of Cu(II), as its complexes are known to

catalyze oxidation reactions, including the oxidation of catechol [116, 117]. The results obtained may open up the possibility of creating selective systems for metal ions separation and may also potentially lead to antimicrobial, antioxidant, and antitumor substances and compositions.

Supplementary materials

This manuscript contains supplementary materials, which are available on the corresponding online page.

Table S1 Crystallographic data and structural refinements of the compound $[\text{Cu}_2(\text{LB})_2(\text{MeOH})_2](\text{TFSI})_2$

Figure S1 Comparison of the experimental powder pattern (room temperature) of the stored sample $[\text{Cu}_2(\text{LB})_2(\text{MeOH})_2](\text{TFSI})_2$ and simulated powder pattern from the single crystal measurement at 300 K.

Figure S2 Experimental and simulated EPR spectra of $[\text{Cu}_2(\text{LE})_2(\text{MeOH})_2](\text{TFSI})_2$ in methanol solution at room temperature. The small signal near 3430 G belongs to a reference radical.

Figure S3 Experimental and simulated second-derivative EPR spectra of $[\text{Cu}_2(\text{LB})_2(\text{MeOH})_2](\text{TFSI})_2$ in methanol solution at room temperature. The small splitting of the high field lines belongs to weak hyperfine coupling with the second nitrogen atom of the ligand's hydrazone moiety. The small signal near 3430 G belongs to a reference radical.

Table S2 EPR spectra parameters.

Data availability statement

The data that support the findings of this study are available from the corresponding author upon reasonable request.

Acknowledgments

We thank Rosa Bikmukhametova for linguistic review and editing of the original manuscript.

Author contributions

Conceptualization: A.B., M.Z., P.P.

Data curation: M.B., Y.K., D.I., A.K., A.G., Z.L., A.R.

Formal Analysis: A.B., M.Z., M.B., Y.K., A.K.

Funding acquisition: P.P.

Investigation: A.B., Y.K., D.I., A.K., A.G., Z.L., A.R.

Methodology: A.B., M.Z., M.B., A.K., P.P.

Project administration: P.P., I.S.

Resources: Y.K., D.I., A.K., A.G., A.R., P.P., I.S.

Supervision: P.P., I.S.

Validation: M.Z., M.B., D.I., A.K.

Visualization: A.B., M.Z., M.B., Y.K.

Writing – original draft: A.B., M.Z., M.B., Y.K.

Writing – review & editing: A.B., M.Z., P.P., I.S.

Conflict of interest

The authors declare no conflict of interest.

Given that Dr. Pavel Padnya acts as an Editor, he was not involved in the peer review of this manuscript. Full responsibility for the editorial process for this submission was delegated to the Editor-in-Chief.

Additional information

Author Scopus IDs:

Azamat Bikmukhametov, [57981814900](https://orcid.org/57981814900)

Maksim Zhernakov, [57877679900](https://orcid.org/57877679900)

Mikhail Bukharov, [54895268200](https://orcid.org/54895268200)

Yury Kuzin, [56732867700](https://orcid.org/56732867700)

Daut Islamov, [15128759500](https://orcid.org/15128759500)

Artur Khannanov, [56037295000](https://orcid.org/56037295000)

Alexander Gerasimov, [40661183600](https://orcid.org/40661183600)

Zubaidullina Liana, [58120259900](https://orcid.org/58120259900)

Alexander Rodionov, [55838511037](https://orcid.org/55838511037)

Pavel Padnya, [26537837000](https://orcid.org/26537837000)

Ivan Stoikov, [6602887534](https://orcid.org/6602887534)

Websites:

Kazan Federal University, <https://kpfu.ru/Eng/>;
 FRC Kazan Scientific Center of the Russian Academy of Sciences,
<https://knc.ru/en>;
 Justus Liebig University Giessen, <https://www.uni-giessen.de/en>.

References

- Bureš F. Quaternary Ammonium Compounds: Simple in Structure, Complex in Application. *Top Curr Chem.* 2019;377(3):14. doi:10.1007/s41061-019-0239-2
- Ohno H. Functional Design of Ionic Liquids. *Bull Chem Soc Japan.* 2006;79(11):1665–80. doi:10.1246/bcsj.79.1665
- Pârvulescu VI, Hardacre C. Catalysis in Ionic Liquids. *Chem Rev.* 2007;107(6):2615–65. doi:10.1021/cro50948h
- Patel DD, Lee J. Applications of ionic liquids. *Chem Rec.* 2012;12(3):329–55. doi:10.1002/tcr.201100036
- Niu H, Wang L, Guan P, Zhang N, Yan C, Ding M, Guo X, Huang T, Hu X. Recent Advances in Application of Ionic Liquids in Electrolyte of Lithium Ion Batteries. *J Energy Storage.* 2021;40:102659. doi:10.1016/j.est.2021.102659
- Singh SK, Savoy AW. Ionic liquids synthesis and applications: An overview. *J Mol Liq.* 2020;297:112038. doi:10.1016/j.molliq.2019.112038
- Karimi B, Tavakolian M, Akbari M, Mansouri F. Ionic Liquids in Asymmetric Synthesis: An Overall View from Reaction Media to Supported Ionic Liquid Catalysis. *ChemCatChem.* 2018;10(15):3173–3205. doi:10.1002/cctc.201701919
- Tang B, Bi W, Tian M, Row KH. Application of ionic liquid for extraction and separation of bioactive compounds from plants. *J Chromatogr B.* 2012;904:1–21. doi:10.1016/j.jchromb.2012.07.020
- Zhuo Y, Cheng H, Zhao Y, Cui H. Ionic Liquids in Pharmaceutical and Biomedical Applications: A Review. *Pharmaceutics.* 2024;16(1):151. doi:10.3390/pharmaceutics16010151
- Greer AJ, Jacquemin J, Hardacre C. Industrial Applications of Ionic Liquids. *Molecules.* 2020;25(21):5207. doi:10.3390/molecules25215207
- Plechko NV, Seddon KR. Applications of ionic liquids in the chemical industry. *Chem Soc Rev.* 2008;37(1):123–50. doi:10.1039/B006677J
- Encyclopedia of Ionic Liquids. Springer Nature Singapore Pte Ltd. 2022. doi:10.1007/978-981-33-4221-7.
- Tindale JJ, Hartlen KD, Alizadeh A, Workentin MS, Ragogna PJ. Maleimide-Modified Phosphonium Ionic Liquids: A Template Towards (Multi)Task-Specific Ionic Liquids. *Chem - Eur J.* 2010;16(30):9068–75. doi:10.1002/chem.200902610
- Gélinas B, Das D, Rochefort D. Air-Stable, Self-Bleaching Electrochromic Device Based on Viologen- and Ferrocene-Containing Triflimide Redox Ionic Liquids. *ACS Appl Mater Interfaces.* 2017;9(34):28726–36. doi:10.1021/acsami.7b04427
- Bhowmik PK, Chen SL, Han H, Ishak KA, Selvi velayutham T, Bendaoud U, Martinez-Felipe A. Dicationic ionic liquids based on bis(4-oligoethoxyphenyl) viologen bistriflimide salts exhibiting high ionic conductivities. *J Mol Liq.* 2022;365:120126. doi:10.1016/j.molliq.2022.120126
- Handa M, Almalki WH, Shukla R, Afzal O, Altamimi AS, Beg S, Rahman M. Active pharmaceutical ingredients (APIs) in ionic liquids: An effective approach for API physicochemical parameter optimization. *Drug Discov Today.* 2022;27(9):2415–24. doi:10.1016/j.drudis.2022.06.003
- Bakulina O, Ivanov M, Alimov D, Prikhod'ko S, Adonin N, Fedin M. Active Pharmaceutical Ingredient-Ionic Liquids (API-ILs): Nanostructure of the Glassy State Studied by Electron Paramagnetic Resonance Spectroscopy. *Molecules.* 2022;27(16):5117. doi:10.3390/molecules27165117
- Belyakova YY, Yaremenko IA, Terent'ev AO, Nenajdenko VG, Shambalova VE, Aldoshin AS, Krasnovskaya OO, Beloglazkina EK, Spektor DV, Machulkin AE, Averin AD, Beletskaya IP, Gromov SP, Magdesieva TV, Fomina MV, Nuriyev VN, Trifonov AA, Loginov DA, Shifrina ZB, Fedorova OA, Fedotova EA, Kuzmina NS, Otvagin VF, Fedorov AY, Kalinin AA, Balakina MY, Aleksandrova YI, Shurpik DN, Stoikov II, Bazhin DN, Burgart YV, Saloutin VI, Korotaev VY, Zimnitsky NS, Ulitko MV, Sosnovskikh VY, Vasilyev AV, Volcho KP, Tikhonov AY, Shelkovnikov VV, Fisyuk AS, Kostyuchenko AS, Shatsauskas AL, Arsenyev MV, Tarakanova AE, Chesnokov SA, Klimochkin YN, Reznikov AN, Ivleva EA, Filimonov VD, Khlebnikov AI, Krasnokutskaya EA, Izmet'ev ES, Lezina OM, Popova SA, Chukicheva IY, Musalov MV, Amosova SV, Potapov VA, Kuimov VA, Fattakhov RI, Belogorlova NA, Parshina LN, Grishchenko LA, Trofimov BA, Adamovich SN, Oborina EN, Zlotzky SS, Raskildina GZ, Sultanova RM, Aksenov AV, Aksenov DA, Aksenov NA, Shikhaliev KS, Stolpovskaya NV, Medvedeva SM, Konshina DN, Konshin VV, Vernigora AA, Burmistrov VV, Novakov IA, Kustova TP, Naumova IK, Kalmykova AA, Dyachenko IV, Dyachenko VD, Grinev VS, Krivenko AP, Yegorova AY, Dotsenko VV, Bespalov AV, Varzieva EA, Kindop VK, Akhmedov AA, Padnya PL, Shiabiev IE, Nazarova AA, Ustynyuk YA. Organic Chemistry in the Creation of Molecules with Practically Useful Properties. *Russ J Gen Chem.* 2026;96(1):1. doi:10.1134/S1070363225605721
- Shukla MK, Tiwari H, Verma R, Dong W, Azizov S, Kumar B, Pandey S, Kumar D. Role and Recent Advancements of Ionic Liquids in Drug Delivery Systems. *Pharmaceutics.* 2023;15(2):702. doi:10.3390/pharmaceutics15020702
- Pedro SN, Freire CS, Silvestre AJ, Freire MG. Ionic Liquids in Drug Delivery. *Encyclopedia.* 2021;1(2):324–39. doi:10.3390/encyclopedia1020027
- Fedorova OV, Ovchinnikova IG, Rusinov GL, Avdeeva VV, Zhdanov AP, Zhizhin KY, Kuznetsov NT, Zakharova LY, Kuznetsova DA, Razuvaeva YS, Zhiltsova EP, Sinyashin OG, Alekseeva AS, Vodovozova EL, Abdrakhmanova II, Ibrahim A, Solovyeva VV, Maltsev AV, Fisenko VP, Bachurin SO, Mikhailov YM, Aleksandrova YI, Shurpik DN, Stoikov II, Ziganshina AY, Solovieva SE, Antipin IS, Agafonov MA, Terekhova IV, Ilicheva PM, Pidenko PS, Burmistrova NA, Moustafine RI, Timergaliev VR, Zabolotnaya YN, Khutoryanskiy VV, Demin AM, Levit GL, Charushin VN, Krasnov VP, Goryacheva OA, Mayorova OA, Mesheryakova SM, Goryacheva IY, Ayupova AI, Fattakhova AA, Rizvanov AA, Inozemtseva OA, Gusliakova OI, Gorin DA, Gerasimov AV, Zubaidullina LS, Ziganshin MA, Valiulin SV, Onischuk AA, Bezrukov AN, Galymetdinov YG, Padnya PL, Nazarova AA, Sultanova ED, Buriyov VA. Modern Strategies of Drug Therapy: Multi-Target Drug Delivery, Bioimaging, Diagnostics. *Russ J Gen Chem.* 2025;95(S1):S1–S448. doi:10.1134/S1070363225606726
- Nikfarjam N, Ghomi M, Agarwal T, Hassanpour M, Sharifi E, Khorsandi D, Ali khan M, Rossi F, Rossetti A, Nazarzadeh zare E, Rabiee N, Afshar D, Vosough M, Kumar maiti T, Matoli V, Lichtfouse E, Tay FR, Makvandi P. Antimicrobial Ionic Liquid-Based Materials for Biomedical Applications. *Adv Funct Mater.* 2021;31(42):2104148. doi:10.1002/adfm.202104148
- Anvari S, Hajfarajollah H, Mokhtarani B, Enayati M, Sharifi A, Mirzaei M. Antibacterial and anti-adhesive properties of ionic liquids with various cationic and anionic heads toward pathogenic bacteria. *J Mol Liq.* 2016;221:685–90. doi:10.1016/j.molliq.2016.05.093
- García MT, Bautista E, De la fuente A, Pérez L. Cholinium-Based Ionic Liquids as Promising Antimicrobial Agents in Pharmaceutical Applications: Surface Activity, Antibacterial Activity and Ecotoxicological Profile. *Pharmaceutics.* 2023;15(7):1806. doi:10.3390/pharmaceutics15071806
- Berthod A, Ruiz-Ángel M, Carda-Broch S. Ionic liquids in separation techniques. *J Chromatogr A.* 2008;1184(1–2):6–18. doi:10.1016/j.chroma.2007.11.109

26. Branco LC, Crespo JG, Afonso CA. Highly Selective Transport of Organic Compounds by Using Supported Liquid Membranes Based on Ionic Liquids. *Angew Chemie Int Ed.* 2002;41(15):2771-3. doi:[doi:10.1002/1521-3773\(20020802\)41:15](https://doi.org/10.1002/1521-3773(20020802)41:15)
27. Han D, Row KH. Recent Applications of Ionic Liquids in Separation Technology. *Molecules.* 2010;15(4):2405-26. doi:[doi:10.3390/molecules15042405](https://doi.org/10.3390/molecules15042405)
28. Wei G, Yang Z, Chen C. Room temperature ionic liquid as a novel medium for liquid/liquid extraction of metal ions. *Anal Chim Acta.* 2003;488(2):183-92. doi:[doi:10.1016/S0003-2670\(03\)00660-3](https://doi.org/10.1016/S0003-2670(03)00660-3)
29. Makanyire T, Sanchez-Segado S, Jha A. Separation and recovery of critical metal ions using ionic liquids. *Adv Manuf.* 2016;4(1):33-46. doi:[doi:10.1007/s40436-015-0132-3](https://doi.org/10.1007/s40436-015-0132-3)
30. H. davis J. Task-Specific Ionic Liquids. *Chem Lett.* 2004;33(9):1072-7. doi:[doi:10.1246/cl.2004.1072](https://doi.org/10.1246/cl.2004.1072)
31. Giernoth R. Task-Specific Ionic Liquids. *Angew Chemie Int Ed.* 2010;49(16):2834-9. doi:[doi:10.1002/anie.200905981](https://doi.org/10.1002/anie.200905981)
32. Menyo MS, Hawker CJ, Waite JH. Versatile tuning of supramolecular hydrogels through metal complexation of oxidation-resistant catechol-inspired ligands. *Soft Matter.* 2013;9(43):10314. doi:[doi:10.1039/C3SM51824H](https://doi.org/10.1039/C3SM51824H)
33. Yan G, Chen G, Peng Z, Shen Z, Tang X, Sun Y, Zeng X, Lin L. The Cross-Linking Mechanism and Applications of Catechol-Metal Polymer Materials. *Adv Mater Interfaces.* 2021;8(19):2100239. doi:[doi:10.1002/admi.202100239](https://doi.org/10.1002/admi.202100239)
34. An Z, Sun J, Mei Q, Wei B, Li M, Xie J, He M, Wang Q. Unravelling the effects of complexation of transition metal ions on the hydroxylation of catechol over the whole pH region. *J Environ Sci.* 2022;115:392-402. doi:[doi:10.1016/j.jes.2021.08.011](https://doi.org/10.1016/j.jes.2021.08.011)
35. Gökçe C, Gup R. Copper(II) complexes of acylhydrazones: synthesis, characterization and DNA interaction. *Appl Organomet Chem.* 2013;27(5):263-8. doi:[doi:10.1002/aoc.2955](https://doi.org/10.1002/aoc.2955)
36. Al-Ne'Aimi MM, Al-Khuder MM. Synthesis, characterization and extraction studies of some metal (II) complexes containing (hydrazonoxime and bis-acylhydrazone) moieties. *Spectrochim Acta Part A: Molecular and Biomolecular Spectroscopy.* 2013;105:365-73. doi:[doi:10.1016/j.saa.2012.10.046](https://doi.org/10.1016/j.saa.2012.10.046)
37. Gup R, Kirkan B. Synthesis and spectroscopic studies of mixed-ligand and polymeric dinuclear transition metal complexes with bis-acylhydrazone tetradentate ligands and 1,10-phenanthroline. *Spectrochim Acta Part A: Molecular and Biomolecular Spectroscopy.* 2006;64(3):809-15. doi:[doi:10.1016/j.saa.2005.08.008](https://doi.org/10.1016/j.saa.2005.08.008)
38. Ahmed MA, Zhernakov MA, Gilyazetdinov EM, Bukharov MS, Islamov DR, Usachev KS, Klimovitskii AE, Serov NY, Burilov VA, Shtyrlin VG. Complexes of NiII, CoII, ZnII, and CuII with Promising Anti-Tuberculosis Drug: Solid-State Structures and DFT Calculations. *Inorganics.* 2023;11(4):167. doi:[doi:10.3390/inorganics11040167](https://doi.org/10.3390/inorganics11040167)
39. Zhang Y, Yan Y, Yang R, Chen R, Dong W. Exploring the structure, fluorescence properties and theoretical studies of newly synthesized Co(II), Ni(II) and Cd(II) complexes bearing acylhydrazone ligands. *J Mol Struct.* 2024;1314:138840. doi:[doi:10.1016/j.molstruc.2024.138840](https://doi.org/10.1016/j.molstruc.2024.138840)
40. Mathew N, Sithambaresan M, Kurup MP. Spectral studies of copper(II) complexes of tridentate acylhydrazone ligands with heterocyclic compounds as coligands: X-ray crystal structure of one acylhydrazone copper(II) complex. *Spectrochim Acta Part A: Molecular and Biomolecular Spectroscopy.* 2011;79(5):1154-61. doi:[doi:10.1016/j.saa.2011.04.036](https://doi.org/10.1016/j.saa.2011.04.036)
41. Lukov VV, Tupolova YP, Kogan VA, Popov LD. Mono- and Binuclear Copper(II) Metal Chelates with 3,5-Di(tert-butyl)salicylaldehyde Acylhydrazones. *Russ J Coord Chem.* 2003;29(5):335-8. doi:[doi:10.1023/A:1023675801876](https://doi.org/10.1023/A:1023675801876)
42. Lukov VV, Knysh AA, Lyubchenko SN, Tupolova YP, Kogan VA. Physicochemical Study of New Mono- and Binuclear Copper(II) Complexes with Sterically Hindered Acylhydrazones and Azomethines. *Russ J Coord Chem.* 2002;28(12):874-6. doi:[doi:10.1023/A:1021642530810](https://doi.org/10.1023/A:1021642530810)
43. Yu M, Liu X, Ren J, Liu J, Yang Z, Zhao S. Thermal properties and CT-DNA/BSA binding behavior of a binuclear Cu(II) complex with acylhydrazone containing naphthalene ring. *J Coord Chem.* 2018;71(7):1020-34. doi:[doi:10.1080/00958972.2018.1457145](https://doi.org/10.1080/00958972.2018.1457145)
44. Wu Y, Wu D, Lan J, Li A, Hou L, Xu Y, Gou Y. Assessment of Mononuclear/Dinuclear Copper acylhydrazone complexes for lung cancer treatment. *Bioorganic Chem.* 2024;144:107122. doi:[doi:10.1016/j.bioorg.2024.107122](https://doi.org/10.1016/j.bioorg.2024.107122)
45. Santiago PH, Duarte ED, Nascimento ÉC, Martins JB, Castro MS, Gatto CC. A binuclear copper(II) complex based on hydrazone ligand: Characterization, molecular docking, and theoretical and antimicrobial investigation. *Appl Organomet Chem.* 2022;36(1):e6461. doi:[doi:10.1002/aoc.6461](https://doi.org/10.1002/aoc.6461)
46. Vrdoljak V, Pavlović G, Maltar-Strmečki N, Cindrić M. Copper(ii) hydrazone complexes with different nuclearities and geometries: synthetic methods and ligand substituent effects. *New J Chem.* 2016;40(11):9263-74. doi:[doi:10.1039/C6NJ01036A](https://doi.org/10.1039/C6NJ01036A)
47. Turomsha I, Gvozdev M, Khodosovskaya A, Sokolova A, Osipovich N, Ksendzova G, Koval'Chuk-Rabchinskaya T, Loginova N. Copper(II) Complexes of Hydrazone and Thiosemicarbazone Ligands: Synthesis, Characterization, Antibacterial and Antifungal Activity. *Chem Porc.* 2025; 18(1): 11. doi:[doi:10.3390/ecsoc-29-26698](https://doi.org/10.3390/ecsoc-29-26698)
48. Bulanov AO, Luk'Yanov BS, Kogan VA, Lukov VV. Binuclear Copper(II) Complexes with Hydrazones Containing Spiropyran Fragment. *Russ J Coord Chem.* 2003;29(9):658-9. doi:[doi:10.1023/A:1025667812707](https://doi.org/10.1023/A:1025667812707)
49. Baryshnikova SV, Arsen'Ev MV, Rumyantsev RV, Yakushev IA, Poddel'Skii AI. Copper(II) o-Iminophenolate Complexes Based on Catecholaldimines. *Russ J Coord Chem.* 2023;49(7):429-36. doi:[doi:10.1134/S107032842360016X](https://doi.org/10.1134/S107032842360016X)
50. Vojinović-Ješić LS, Bogdanović GA, Leovac VM, Češljević VI, Jovanović LS. Transition metal complexes with Girard reagent-based ligands. Part IV. Synthesis and characterization of pyridoxilidene Girard-T hydrazone complexes. Crystal structure of the copper(II) complex. *Struct Chem.* 2008;19(5):807-15. doi:[doi:10.1007/s11224-008-9368-x](https://doi.org/10.1007/s11224-008-9368-x)
51. Leovac VM, Bogdanović GA, Češljević VI, Jovanović LS, Novaković SB, Vojinović-Ješić LS. Transition metal complexes with Girard reagent-based ligands. *Struct Chem.* 2007;18(1):113-9. doi:[doi:10.1007/s11224-006-9136-8](https://doi.org/10.1007/s11224-006-9136-8)
52. Sreenivasulu R, Reddy KT, Sujitha P, Kumar CG, Raju RR. Synthesis, antiproliferative and apoptosis induction potential activities of novel bis(indolyl)hydrazide-hydrazone derivatives. *Bioorganic Med Chem.* 2019;27(6):1043-55. doi:[doi:10.1016/j.bmc.2019.02.002](https://doi.org/10.1016/j.bmc.2019.02.002)
53. Li Y, Yan W, Yang J, Yang Z, Hu M, Bai P, Tang M, Chen L. Discovery of novel β -carboline/acylhydrazone hybrids as potent antitumor agents and overcome drug resistance. *Eur J Med Chem.* 2018;152:516-26. doi:[doi:10.1016/j.ejmech.2018.05.003](https://doi.org/10.1016/j.ejmech.2018.05.003)
54. Lis C, Rubner S, Roatsch M, Berg A, Gilcrest T, Fu D, Nguyen E, Schmidt A, Krautscheid H, Meiler J, Berg T. Development of Erasin: a chromone-based STAT3 inhibitor which induces apoptosis in Erlotinib-resistant lung cancer cells. *Sci Reports.* 2017;7(1):17390. doi:[doi:10.1038/s41598-017-17600-x](https://doi.org/10.1038/s41598-017-17600-x)
55. Bonnett SA, Dennison D, Files M, Bajpai A, Parish T. A class of hydrazones are active against non-replicating Mycobacterium tuberculosis. *Plos One.* 2018;13(10):e0198059. doi:[doi:10.1371/journal.pone.0198059](https://doi.org/10.1371/journal.pone.0198059)
56. Guilherme FD, Simonetti JÉ, Folquitto LR, Reis AC, Oliver JC, Dias AL, Dias DF, Carvalho DT, Brandão GC, Souza TB. Synthesis, chemical characterization and antimicrobial activity of new acylhydrazones derived from carbohydrates. *J Mol Struct.* 2019;1184:349-56. doi:[doi:10.1016/j.molstruc.2019.02.045](https://doi.org/10.1016/j.molstruc.2019.02.045)

57. Reznichenko O, Quillévéré A, Martins RP, Loaç N, Kang H, Lista MJ, Beauvineau C, González-García J, Guillot R, Vissot C, Daskalogianni C, Fähræus R, Teulade-Fichou M, Blondel M, Granzhan A. Novel cationic bis(acylhydrazones) as modulators of Epstein–Barr virus immune evasion acting through disruption of interaction between nucleolin and G-quadruplexes of EBNA1 mRNA. *Eur J Med Chem.* 2019;178:13–29. doi:[doi:10.1016/j.ejmech.2019.05.042](https://doi.org/10.1016/j.ejmech.2019.05.042)
58. Dos santos filho JM, De queiroz e silva DM, Macedo TS, Teixeira HM, Moreira DR, Challal S, Wolfender J, Queiroz EF, Soares MB. Conjugation of N-acylhydrazone and 1,2,4-oxadiazole leads to the identification of active antimalarial agents. *Bioorganic Med Chem.* 2016;24(22):5693–5701. doi:[doi:10.1016/j.bmc.2016.09.013](https://doi.org/10.1016/j.bmc.2016.09.013)
59. Wani MY, Bhat AR, Azam A, Athar F. Nitroimidazolyl hydrazones are better amoebicides than their cyclized 1,3,4-oxadiazoline analogues: In vitro studies and Lipophilic efficiency analysis. *Eur J Med Chem.* 2013;64:190–9. doi:[doi:10.1016/j.ejmech.2013.03.034](https://doi.org/10.1016/j.ejmech.2013.03.034)
60. Massarico serafim RA, Gonçalves JE, De souza FP, De melo loureiro AP, Storpirtis S, Krogh R, Andricopulo AD, Dias LC, Ferreira EI. Design, synthesis and biological evaluation of hybrid bioisoster derivatives of N-acylhydrazone and furaxan groups with potential and selective anti-Trypanosoma cruzi activity. *Eur J Med Chem.* 2014;82:418–25. doi:[doi:10.1016/j.ejmech.2014.05.077](https://doi.org/10.1016/j.ejmech.2014.05.077)
61. Cerqueira JV, Meira CS, Santos ED, De aragão França LS, Vasconcelos JF, Nonaka CK, De melo TL, Dos santos filho JM, Moreira DR, Soares MB. Anti-inflammatory activity of SintMed65, an N-acylhydrazone derivative, in a mouse model of allergic airway inflammation. *Int Immunopharmacol.* 2019;75:105735. doi:[doi:10.1016/j.intimp.2019.105735](https://doi.org/10.1016/j.intimp.2019.105735)
62. Moraes AD, Miranda MD, Jacob ÍT, Amorim CA, Moura RO, Silva SÂ, Soares MB, Almeida SM, Souza TR, Oliveira JF, Silva TG, Melo CM, Moreira DR, Lima MD. Synthesis, in vitro and in vivo biological evaluation, COX-1/2 inhibition and molecular docking study of indole-N-acylhydrazone derivatives. *Bioorganic Med Chem.* 2018;26(20):5388–96. doi:[doi:10.1016/j.bmc.2018.07.024](https://doi.org/10.1016/j.bmc.2018.07.024)
63. Duarte CD, Tributino JL, Lacerda DI, Martins MV, Alexandre-Moreira MS, Dutra F, Bechara EJ, De-Paula FS, Goulart MO, Ferreira J, Calixto JB, Nunes MP, Bertho AL, Miranda AL, Barreiro EJ, Fraga CA. Synthesis, pharmacological evaluation and electrochemical studies of novel 6-nitro-3,4-methylenedioxyphenyl-N-acylhydrazone derivatives: Discovery of LASSBio-881, a new ligand of cannabinoid receptors. *Bioorganic Med Chem.* 2007;15(6):2421–33. doi:[doi:10.1016/j.bmc.2007.01.013](https://doi.org/10.1016/j.bmc.2007.01.013)
64. Zhan K, Ejima H, Yoshie N. Antioxidant and Adsorption Properties of Bioinspired Phenolic Polymers: A Comparative Study of Catechol and Gallol. *ACS Sustain Chem Eng.* 2016;4(7):3857–63. doi:[doi:10.1021/acssuschemeng.6b00626](https://doi.org/10.1021/acssuschemeng.6b00626)
65. Smolyaninov IV, Burmistrova DA, Arsenyev MV, Polovinkina MA, Pomortseva NP, Fukin GK, Poddel'Sky AI, Berberova NT. Synthesis and Antioxidant Activity of New Catechol Thi-oethers with the Methylene Linker. *Molecules.* 2022;27(10):3169. doi:[doi:10.3390/molecules27103169](https://doi.org/10.3390/molecules27103169)
66. Hasegawa U, Moriyama M, Uyama H, Van der vliet AJ. Catechol-bearing block copolymer micelles: Structural characterization and antioxidant activity. *Polymer.* 2015;66:1–7. doi:[doi:10.1016/j.polymer.2015.03.080](https://doi.org/10.1016/j.polymer.2015.03.080)
67. Saiz-poseu J, Mancebo-aracil J, Nador F, Busqué F, Ruiz-molina D. The Chemistry behind Catechol-Based Adhesion. *Angew Chemie Int Ed.* 2019;58(3):696–714. doi:[doi:10.1002/anie.201801063](https://doi.org/10.1002/anie.201801063)
68. Zhang W, Wang R, Sun Z, Zhu X, Zhao Q, Zhang T, Cholewinski A, Yang F, Zhao B, Pinnaratip R, Forooshani PK, Lee BP. Catechol-functionalized hydrogels: biomimetic design, adhesion mechanism, and biomedical applications. *Chem Soc Rev.* 2020;49(2):433–64. doi:[doi:10.1039/C9CS00285E](https://doi.org/10.1039/C9CS00285E)
69. Moulay S. Dopa/Catechol-Tethered Polymers: Bioadhesives and Biomimetic Adhesive Materials. *Polym Rev.* 2014;54(3):436–513. doi:[doi:10.1080/15583724.2014.881373](https://doi.org/10.1080/15583724.2014.881373)
70. Nadagouda MN, Vijayarathy P, Sin A, Nam H, Khan S, Parambath JB, Mohamed AA, Han C. Antimicrobial activity of quaternary ammonium salts: structure-activity relationship. *Med Chem Res.* 2022;31(10):1663–78. doi:[doi:10.1007/s00044-022-02924-9](https://doi.org/10.1007/s00044-022-02924-9)
71. Zhou Z, Zhou S, Zhang X, Zeng S, Xu Y, Nie W, Zhou Y, Xu T, Chen P. Quaternary Ammonium Salts: Insights into Synthesis and New Directions in Antibacterial Applications. *Bioconjugate Chem.* 2023;34(2):302–25. doi:[doi:10.1021/acs.bioconjchem.2c00598](https://doi.org/10.1021/acs.bioconjchem.2c00598)
72. Dan W, Gao J, Qi X, Wang J, Dai J. Antimicrobial quaternary ammonium agents: Chemical diversity and biological mechanism. *Eur J Med Chem.* 2022;243:114765. doi:[doi:10.1016/j.ejmech.2022.114765](https://doi.org/10.1016/j.ejmech.2022.114765)
73. Bogdanov AV, Tagasheva RG, Voloshina A, Lyubina A, Tsivileva O, Kuzovlev AN, Yi W, Samorodov AV, Ziyatdinova GK, Zhiganshina ER, Arsenyev MV, Bukharov SV. Ammonium Catecholaldehydes as Multifunctional Bioactive Agents: Evaluating Antimicrobial, Antioxidant, and Antiplatelet Activity. *Int J Mol Sci.* 2025;26(16):7866. doi:[doi:10.3390/ijms26167866](https://doi.org/10.3390/ijms26167866)
74. Bogdanov AV, Bukharov SV, Garifullina RA, Voloshina AD, Lyubina AP, Amerkhanova SK, Bezzonova MS, Khaptsev ZY, Tsivileva OM. Synthesis and Antimicrobial Activity Evaluation of Ammonium Acylhydrazones Based on 4,6-Di-tert-butyl-2,3-dihydroxybenzaldehyde. *Russ J Gen Chem.* 2022;92(10):1875–86. doi:[doi:10.1134/S1070363222100012](https://doi.org/10.1134/S1070363222100012)
75. Neganova M, Aleksandrova Y, Voloshina A, Lyubina A, Ap-pazov N, Yespenbetova S, Valiullina Z, Samorodov A, Bukharov S, Gibadullina E, Tapalova A, Bogdanov A. Biological Activity Evaluation of Phenolic Isatin-3-Hydrazones Containing a Quaternary Ammonium Center of Various Structures. *Int J Mol Sci.* 2024;25(20):11130. doi:[doi:10.3390/ijms252011130](https://doi.org/10.3390/ijms252011130)
76. Bogdanov AV, Iskhakova KR, Voloshina AD, Sapunova AS, Kulik NV, Terekhova NV, Arsenyev MV, Ziyatdinova GK, Bukharov SV. Ammonium-Charged Sterically Hindered Phenols with Antioxidant and Selective Anti-Gram-Positive Bacterial Activity. *Chem Biodivers.* 2020;17(5):e2000147. doi:[doi:10.1002/cbdv.202000147](https://doi.org/10.1002/cbdv.202000147)
77. Bogdanov AV, Samorodov AV, Valiullina ZA, Akyzbekov NI, Voloshina AD, Lyubina AP, Amerkhanova SK, Saitova AM, Pashirova TN, Tsivileva OM, Mironov VF. Biologically Active Ammonium Isatin-3-acylhydrazones Bearing Long-Chain Alkyl Substituent of Various Structures. *Russ J Gen Chem.* 2024;94(3):539–52. doi:[doi:10.1134/S1070363224030071](https://doi.org/10.1134/S1070363224030071)
78. Bogdanov AV, Bukharov SV, Yusupov AN, Litvinov IA, Voloshina AD, Tagasheva RG, Kolpakova EV. Ammonium acylhydrazones based on 4,6-di-tert-butyl-2,3-dihydroxybenzaldehyde: synthesis, possibilities of functionalization, and evaluation of biological activity. *Russ Chem Bull.* 2024;73(3):704–13. doi:[doi:10.1007/s11172-024-4181-2](https://doi.org/10.1007/s11172-024-4181-2)
79. Bogdanov AV, Voloshina AD, Sapunova AS, Kulik NV, Bukharov SV, Dobrynin AB, Voronina JK, Terekhova NV, Samorodov AV, Pavlov VN, Mironov VF. Isatin-3-acylhydrazones with Enhanced Lipophilicity: Synthesis, Antimicrobial Activity Evaluation and the Influence on Hemostasis System. *Chem Biodivers.* 2022;19(2):e202100496. doi:[doi:10.1002/cbdv.202100496](https://doi.org/10.1002/cbdv.202100496)
80. Bogdanov AV, Zaripova IF, Mustafina LK, Voloshina AD, Sapunova AS, Kulik NV, Mironov VF. Synthesis and Study of Antimicrobial Activity of Water-Soluble Ammonium Acylhydrazones Based on New 1,ω-Alkylenebis(isatins). *Russ J Gen Chem.* 2019;89(7):1368–76. doi:[doi:10.1134/S107036321907003X](https://doi.org/10.1134/S107036321907003X)
81. Bogdanov AV, Kadomtseva ME, Bukharov SV, Voloshina AD, Mironov VF. Effect of the Cationic Moiety on the Antimicro-

- bial Activity of Sterically Hindered Isatin 3-Hydrazone Derivatives. *Russ J Org Chem.* 2020;56(3):555–8. doi:[doi:10.1134/S107042802003032X](https://doi.org/10.1134/S107042802003032X)
82. Shaihtudinova Z, Vandyukov A, Lushchekina S, Mironov V, Bukharov S, Tagasheva R, Bogdanov A, Arsenyev M, Masson P, Pashirova T. Amphiphilic ammonium acylhydrazones on the base of sterically-hindered catechol: Synthesis, self-assembly, reversible inhibition of butyrylcholinesterase and structure-activity relationships. *J Mol Liq.* 2025;437:128360. doi:[doi:10.1016/j.molliq.2025.128360](https://doi.org/10.1016/j.molliq.2025.128360)
83. Moseev TD, Varaksin MV, Krinochkin AP, Valieva MA, Kudryashova EA, Sayfutdinova YM, Rybakova AV, Kopchuk DS, Zyryanov GV, Ballou Y, Slepukhin PA, Gaviko VS, Charushin VN, Chupakhin ON. Copper(II) complexes with fluorinated 5-aryl-2,2'-bipyridine-6(6')-carboxylic acid tridentate ligands. *Chim Techno Acta.* 2025;12(2):12217. doi:[doi:10.15826/chimtech.2025.12.2.17](https://doi.org/10.15826/chimtech.2025.12.2.17)
84. Ermolaev AV, Shtyrin VG, Gizatullin AI, Zhernakov MA, Serov NY, Urazaeva KV, Bukharov MS, Gilyazetdinov EM, Islamov DR, Rodionov AA, Mirzayanov II, Garifzyanov AR, Kuramshin BK. Development of comprehensive approaches to characterizing CuII complexes: structures in solution and solid-state, dynamic behavior, and bioactivity. *ChemistrySelect.* 2023;8(48):e202303333. doi:[doi:10.1002/slct.202303333](https://doi.org/10.1002/slct.202303333)
85. Krasnovskaya O, Naumov A, Guk D, Gorelkin P, Erofeev A, Beloglazkina E, Majouga A. Copper Coordination Compounds as Biologically Active Agents. *Int J Mol Sci.* 2020;21(11):3965. doi:[doi:10.3390/ijms21113965](https://doi.org/10.3390/ijms21113965)
86. Hasinoff BB, Wu X, Yadav AA, Patel D, Zhang H, Wang D, Chen Z, Yalowich JC. Cellular mechanisms of the cytotoxicity of the anticancer drug elesclomol and its complex with Cu(II). *Biochem Pharmacol.* 2015;93(3):266–76. doi:[doi:10.1016/j.bcp.2014.12.008](https://doi.org/10.1016/j.bcp.2014.12.008)
87. Zalevskaya OA, Gur'Eva YA. Recent Studies on the Antimicrobial Activity of Copper Complexes. *Russ J Coord Chem.* 2021;47(12):861–80. doi:[doi:10.1134/S1070328421120046](https://doi.org/10.1134/S1070328421120046)
88. Rosu T, Pahontu E, Maxim C, Georgescu R, Stanica N, Gulea A. Some new Cu(II) complexes containing an ON donor Schiff base: Synthesis, characterization and antibacterial activity. *Polyhedron.* 2011;30(1):154–62. doi:[doi:10.1016/j.poly.2010.10.001](https://doi.org/10.1016/j.poly.2010.10.001)
89. Weiskirchen R. Comprehensive Pharmacological Management of Wilson's Disease: Mechanisms, Clinical Strategies, and Emerging Therapeutic Innovations. *Sci.* 2025;7(3):94. doi:[doi:10.3390/sci7030094](https://doi.org/10.3390/sci7030094)
90. Fujisawa C, Kodama H, Sato Y, Mimaki M, Yagi M, Awano H, Matsuo M, Shintaku H, Yoshida S, Takayanagi M, Kubota M, Takahashi A, Akasaka Y. Early clinical signs and treatment of Menkes disease. *Mol Genet Metab Reports.* 2022;31:100849. doi:[doi:10.1016/j.ymgmr.2022.100849](https://doi.org/10.1016/j.ymgmr.2022.100849)
91. Bikmukhametov A, Vasilevskaya N, Arsenyev M, Gerasimov A, Bukharov M, Islamov D, Belyakova S, Kuzin Y, Evtugyn G, Padnya P, Stoikov I. Task-specific ionic liquid and organic salts based on catechol-containing hydrazones: Synthesis, selective Cu(II) binding, thermal properties, and redox-activity. *J Mol Liq.* 2025;425:127234. doi:[doi:10.1016/j.molliq.2025.127234](https://doi.org/10.1016/j.molliq.2025.127234)
92. Sheldrick GM. A short history of SHELX. *Acta Crystallogr Sect Found Crystallogr.* 2008;64(1):112–22. doi:[doi:10.1107/S0108767307043930](https://doi.org/10.1107/S0108767307043930)
93. Sheldrick G. SHELXT: Integrating space group determination and structure solution. *Acta Crystallogr Sect Found Adv.* 2014;70(a1):C1437–7. doi:[doi:10.1107/s2053273314085623](https://doi.org/10.1107/s2053273314085623)
94. Macrae CF, Edgington PR, McCabe P, Pidcock E, Shields GP, Taylor R, Towler M, Van de Streek J. Mercury: visualization and analysis of crystal structures. *J Appl Crystallogr.* 2006;39(3):453–7. doi:[doi:10.1107/S002188980600731X](https://doi.org/10.1107/S002188980600731X)
95. Stoll S, Schweiger A. EasySpin, a comprehensive software package for spectral simulation and analysis in EPR. *J Magn Reson.* 2006;178(1):42–55. doi:[doi:10.1016/j.jmr.2005.08.013](https://doi.org/10.1016/j.jmr.2005.08.013)
96. Hazra S, Martins LM, Guedes da Silva MF, Pombeiro AJ. Sulfonated Schiff base copper(II) complexes as efficient and selective catalysts in alcohol oxidation: syntheses and crystal structures. *RSC Adv.* 2015;5(109):90079–88. doi:[doi:10.1039/C5RA19498A](https://doi.org/10.1039/C5RA19498A)
97. Martins NM, Mahmudov KT, Guedes da Silva MF, Martins LM, Pombeiro AJ. Copper(II) and iron(III) complexes with arylhydrazone of ethyl 2-cyanoacetate or formazan ligands as catalysts for oxidation of alcohols. *New J Chem.* 2016;40(12):10071–83. doi:[doi:10.1039/C6NJ02161A](https://doi.org/10.1039/C6NJ02161A)
98. Böhme M, Mohanty M, Lima S, Buchholz A, Görls H, Dinda R, Plass W. Dinuclear Copper(II) Complex with Intramolecular O–H...O Hydrogen Bonding: Magneto-Structural Correlation for Acylhydrazone-Based Phenoxido Bridged Copper(II) Complexes. *Eur J Inorg Chem.* 2024;27(36):e202400531. doi:[doi:10.1002/ejic.202400531](https://doi.org/10.1002/ejic.202400531)
99. Isaeva ÉL, Shamsutdinova MK, Bukov NN, Panyushkin VT. Composition and magnetic properties of a complex compound of Cu(II) with 2-[2-hydroxyphenyl]-4,4-diphenyl-1,2-dihydro-4h-3,1-benzoxazine. *J Struct Chem.* 2011;52(5):1037–9. doi:[doi:10.1134/S0022476611050349](https://doi.org/10.1134/S0022476611050349)
100. Veidis MV, Schreiber GH, Gough TE, Palenik GJ. Jahn-Teller distortions in octahedral copper(II) complexes. *J Am Chem Soc.* 1969;91(7):1859–60. doi:[doi:10.1021/ja01035a051](https://doi.org/10.1021/ja01035a051)
101. Moura FD, Sobrinho YS, Stellet C, Serna JD, Ligerio CB, Yogui MI, Cukierman DS, Diniz R, Alves OC, Morgon NH, De Souza AR, Rey NA. Copper(II) complexes of a furan-containing arylhydrazone ligand: syntheses, structural studies, solution chemistry and interaction with HSA. *Dalton Trans.* 2023;52(47):17731–46. doi:[doi:10.1039/d3dt02597g](https://doi.org/10.1039/d3dt02597g)
102. Kawano M, Wu Y, Li Z, Mishima A, Kawata S, Ishikawa R. Magnetic superexchange couplings in doubly bis(2-pyridyl)pyrazolato-bridged dinuclear copper(II) complexes. *New J Chem.* 2025;49(36):15691–9. doi:[doi:10.1039/D5NJ02006A](https://doi.org/10.1039/D5NJ02006A)
103. Rojas O, Mirzoyan G, Adamyan Z, Papoyan VV, Amatuni G, Ananikian N. Magnetic properties and entanglement in anti-ferromagnetic interactions in copper(II) dinuclear and trinuclear complexes. *Sci Reports.* 2025;15(1):11758. doi:[doi:10.1038/s41598-025-92130-5](https://doi.org/10.1038/s41598-025-92130-5)
104. Rodríguez MR, Balsa LM, Piro OE, Etcheverría GA, García-Tojal J, Pis-Diez R, León IE, Parajón-Costa BP, González-Baró AC. Synthesis, Crystal Structure, Spectroscopic Characterization, DFT Calculations and Cytotoxicity Assays of a New Cu(II) Complex with an Acylhydrazone Ligand Derived from Thiophene. *Inorganics.* 2021;9(2):9. doi:[doi:10.3390/inorganics9020009](https://doi.org/10.3390/inorganics9020009)
105. Burgos-López Y, Balsa LM, Piro OE, León IE, García-Tojal J, Etcheverría GA, González-Baró AC, Parajón-Costa BS. Tridentate acylhydrazone copper(II) complexes with heterocyclic bases as coligands. Synthesis, spectroscopic studies, crystal structure and cytotoxicity assays. *Polyhedron.* 2022;213:115621. doi:[doi:10.1016/j.poly.2021.115621](https://doi.org/10.1016/j.poly.2021.115621)
106. Kuzin YI, Guseinova A, Bikmukhametov AA, Padnya PL, Stoikov II, Porfireva AV. Electrochemical behavior of catechol-based redox-active ionic liquids and their application in electrochemical sensing of l-cysteine. *Electrochimica Acta.* 2026;564:148737. doi:[doi:10.1016/j.electacta.2026.148737](https://doi.org/10.1016/j.electacta.2026.148737)
107. Jones SE, Chin DH, Sawyer DT. Redox chemistry of metal-catechol complexes in aprotic media. 2. 3,5-Di-tert-butylcatechol complexes of manganese(IV) and manganese(III). *Inorg Chem.* 1981;20(12):4257–62. doi:[doi:10.1021/ic50226a045](https://doi.org/10.1021/ic50226a045)
108. Pashanova KI, Bitkina VO, Yakushev IA, Arsenyev MV, Piskunov AV. Square-Planar Heteroleptic Complexes of α -Diimine-Ni(II)-Catecholate Type: Intramolecular Ligand-to-Ligand Charge Transfer. *Molecules.* 2021;26(15):4622. doi:[doi:10.3390/molecules26154622](https://doi.org/10.3390/molecules26154622)
109. Park I, Tabelin CB, Seno K, Jeon S, Ito M, Hiro Yoshi N. Simultaneous suppression of acid mine drainage formation and arsenic release by carrier-microencapsulation using aluminum-catecholate complexes. *Chemosphere.* 2018;205:414–25. doi:[doi:10.1016/j.chemosphere.2018.04.088](https://doi.org/10.1016/j.chemosphere.2018.04.088)

110. Li X, Hiroyoshi N, Tabelin CB, Naruwa K, Harada C, Ito M. Suppressive effects of ferric-catecholate complexes on pyrite oxidation. *Chemosphere*. 2019;214:70–8. [doi:10.1016/j.chemosphere.2018.09.086](https://doi.org/10.1016/j.chemosphere.2018.09.086)
111. Park I, Tabelin CB, Magaribuchi K, Seno K, Ito M, Hiroyoshi N. Suppression of the release of arsenic from arsenopyrite by carrier-microencapsulation using Ti-catechol complex. *J Hazard Mater*. 2018;344:322–32. [doi:10.1016/j.jhazmat.2017.10.025](https://doi.org/10.1016/j.jhazmat.2017.10.025)
112. Pashanova KI, Ershova IV, Trofimova OY, Rumyantsev RV, Fukin GK, Bogomyakov AS, Arsenyev MV, Piskunov AV. Charge Transfer Chromophores Derived from 3d-Row Transition Metal Complexes. *Molecules*. 2022;27(23):8175. [doi:10.3390/molecules27238175](https://doi.org/10.3390/molecules27238175)
113. Tembwe I, Ngila JC, Kgarebe B, Darkwa J, Iwuoha E. Electrochemical studies of the nickel catecholate complexes for detection of sulphur dioxide gas. *Electrochimica Acta*. 2010;55(14):4314–8. [doi:10.1016/j.electacta.2009.06.081](https://doi.org/10.1016/j.electacta.2009.06.081)
114. Harmalker S, Jones SE, Sawyer DT. Electrochemical and spectroscopic studies of 3,5-di-tert-butylcatecholato and 3,5-di-tert-butyl-o-semiquinonato complexes of copper(II). *Inorg Chem*. 1983;22(20):2790–4. [doi:10.1021/ico0162a005](https://doi.org/10.1021/ico0162a005)
115. Nematollahi D, Golabi S. Electrochemical study of catechol and 4-methylcatechol in methanol. Application to the electro-organic synthesis of 4,5-dimethoxy- and 4-methoxy-5-methyl-o-benzoquinone. *J Electroanal Chem*. 1996;405(1-2):133–40. [doi:10.1016/0022-0728\(95\)04402-7](https://doi.org/10.1016/0022-0728(95)04402-7)
116. Mccann SD, Stahl SS. Copper-Catalyzed Aerobic Oxidations of Organic Molecules: Pathways for Two-Electron Oxidation with a Four-Electron Oxidant and a One-Electron Redox-Active Catalyst. *Accounts Chem Res*. 2015;48(6):1756–66. [doi:10.1021/acs.accounts.5b00060](https://doi.org/10.1021/acs.accounts.5b00060)
117. Gogoi G, Nath JK, Hoque N, Biswas S, Gour NK, Kalita DJ, Bora SR, Bania KK. Single and multiple site Cu(II) catalysts for benzyl alcohol and catechol oxidation reactions. *Appl Catal A: General*. 2022;644:118816. [doi:10.1016/j.apcata.2022.118816](https://doi.org/10.1016/j.apcata.2022.118816)